

AD-A121 427

ON THE RESPONSE OF KNOLLENBERG HEROSOL COUNTERS (U)  
ROYAL AIRCRAFT ESTABLISHMENT FARNBOROUGH (ENGLAND)  
R R ALLAN ET AL. APR 82 RAE-TR-82841 DRIC-BR-84258

UNCLASSIFIED

F/G 14/2

NL

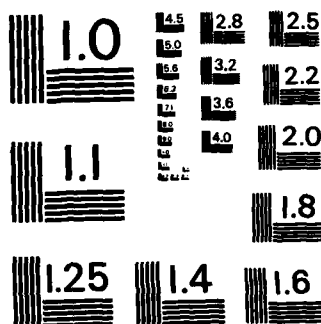


END

FILMED

1

DATE



MICROCOPY RESOLUTION TEST CHART  
NATIONAL BUREAU OF STANDARDS - 1963 - A

③

BR84258  
TR 82041

TR 82041



ROYAL AIRCRAFT ESTABLISHMENT

\*

Technical Report 82041

April 1982

**ON THE RESPONSE OF  
KNOLLENBERG AEROSOL COUNTERS**

by

R. R. Allan  
P. C. Ashdown

\*

DTIC  
ELECTE  
NOV 16 1982  
S D E

Procurement Executive, Ministry of Defence  
Farnborough, Hants

82 11 12 064

DTIC FILE COPY

AD 82041

UDC 541.182.2/3 : 681.785.5 : 535.32

R O Y A L   A I R C R A F T   E S T A B L I S H M E N T

Technical Report 82041

Received for printing 13 April 1982

ON THE RESPONSE OF KNOLLENBERG AEROSOL COUNTERS

by

R. R. Allan

P. C. Ashdown

SUMMARY

It is known that the response of light-scattering aerosol counters is sensitive to the aerosol refractive index, and that even for a given refractive index there are 'multi-valued' regions where significantly different sizes of particle give the same response. In natural aerosols, the particle size distribution inferred directly from measurements shows a 'knee' followed by a sharp drop. Moreover the position of the knee should depend on the aerosol refractive index.

In practice the most obvious feature is a knee near 1  $\mu$ m nominal size on range 0 of the Knollenberg ASAS counter, although further features are present at much poorer resolution on range 1 of the Knollenberg CSAS counter. Here we show that the position of the knee correlates very well with relative humidity and thus with the refractive index. These 'artificial' features can be turned to advantage in field measurements of natural aerosol since they provide a measure of the refractive index.

Departmental Reference: Space 615

Copyright  
©  
Controller HMSO London  
1982



Accession For	
NTIS GRA&I	<input checked="" type="checkbox"/>
DTIC TAB	<input type="checkbox"/>
Unannounced	<input type="checkbox"/>
Justification	
By	
Distribution/	
Availability Codes	
Dist	Avail. and/or Special
A	

LIST OF CONTENTS

	<u>Page</u>
1 INTRODUCTION	3
2 PRINCIPLES	3
3 RESULTS	4
4 CONCLUSIONS	7
References	8
Illustrations	Figures 1-6
Report documentation page	inside back cover

## 1 INTRODUCTION

Pinnick and Auvermann<sup>1</sup> have discussed the response characteristics of various Knollenberg aerosol counters - in particular the active scattering aerosol spectrometer (ASAS) and the classical scattering aerosol spectrometer (CSAS). They stress that the response is sensitive to the aerosol refractive index. Moreover, even with a given refractive index, spherical particles of different sizes can produce the same response in certain regions; these are described as regions of multi-valued response, although it is not the response which is multi-valued but the size of particle to be inferred from a given response.

## 2 PRINCIPLES

Both counters act by collecting the light scattered as each individual particle passes through the beam from a He-Ne laser. The CSAS probe is conceptually simpler since the scattering volume lies outside the optical cavity of the laser. As shown in Fig 1b, the acceptance solid angle of the collecting optics is a hollow cone between half-angles of  $4^\circ$  and  $22^\circ$  off the forward direction of the laser beam - the missing centre of the cone being determined by the presence of a dump spot to stop the direct beam from the laser. In the ASAS 'active' probe (Fig 1a) the dump spot is replaced by a plane mirror so that the scattering volume now lies within the optical cavity of the laser (which now has a Brewster window). The geometry of the collecting optics is otherwise identical to the CSAS, although the particles are now illuminated by light travelling in both directions with consequent interference effects.

Since the acceptance solid angle of the collecting optics is much less than the full  $4\pi$ , it is clear that the *total* scattering cross-section is not strictly applicable. Nevertheless both counters collect a large part of the total scattered light except for particles considerably smaller than the wavelength, when the angular distribution tends to the  $(1 + \cos^2 \theta)$  form, or very much larger than the wavelength when the scattering becomes concentrated about the forward direction. We shall therefore explain the principles underlying the effects of interest by considering the *total* scattering. The theory is conventionally couched in terms of the 'scattering efficiency factor'  $Q_s(x, m)$ , where  $x = 2\pi r/\lambda$ , and  $m = n_1 - in_2$ , where  $n_1$  is the refractive index and  $n_2$  is the absorption. By definition  $Q_s(x, m)$  is the ratio of the total scattering cross-section to the geometrical cross-section  $\pi r^2$ , i.e. the total scattering cross-section is  $\pi r^2 Q_s(x, m)$ .

Born and Wolf<sup>2</sup> state that, provided  $(n_1 - 1)$  is not too large and  $n_2$  is negligible,  $Q_s(x, m)$  is approximately a universal function of  $(n_1 - 1)x$  with its first and largest peak at  $(n_1 - 1)x \approx 2$ . Fig 2 shows the *total* scattering efficiency factors for the refractive indices  $n_1 = 1.3, 1.4, 1.5$  and  $1.6$ , and with negligible absorption, plotted as functions of the dimensionless argument  $(n_1 - 1)x$ . The functions are calculated using a modified form of the standard Mie scatter programmes due to Dave<sup>3</sup>; since the programmes require that  $n_2$  should not be exactly zero, the absorption was taken as  $n_2 = 10^{-8}$ . Clearly Fig 2 confirms the assertion<sup>2</sup> that the gross

forms of the functions are very similar, although there are quite marked small-scale oscillations in the individual curves. Fig 3 similarly shows the *total* scattering cross-section,  $\pi r^2 Q_s(x, m)$ , for the same values of refractive index, now plotted against particle radius assuming  $\lambda = 0.6328 \mu\text{m}$ . The horizontal scale is chosen to include ASAS range 0, namely 0.3 to 1.5  $\mu\text{m}$  radius, and the Y-axis gives the cross-section in units of  $(\mu\text{m})^2$  on a log scale. All the cross-section curves show a plateau or even a slight dip (confused somewhat by the small-scale oscillations), which correspond to the region from the first gross maximum to the first gross minimum of  $Q_s(x, m)$  in Fig 2. It is clear, however, that if the counter were detecting the *total* scattered energy, then a range of particle size in the region of the plateau or dip would give much the same response. Moreover the particle size at which the plateau or dip occurs, and also the response, decrease as the refractive index increases.

It must be emphasised that Figs 2 and 3 are given to illustrate the principles and are not strictly applicable to the Knollenberg counters. The proper calculation of the Knollenberg counter responses is a much longer process which requires the calculation of the scattering angular distribution followed by an integration between the limits imposed by the geometry of the detecting optics. The results of such exact calculations are given by Pinnick and Auvermann<sup>1</sup> in their Figs 13 and 12 for the ASAS and CSAS counters, respectively, for various values of  $m$ :  $m = 1.33 - 0i$  (water),  $m = 1.50 - 0i$  (ammonium sulphate),  $m = 1.50 - 0.005i$  and  $1.50 - 0.05i$  (atmospheric dust) and  $m = 1.95 - 0.66i$  (carbon). They also give results for various calibration substances (polystyrene, glass, nigrosin dye), sodium chloride and potassium chlorate in their Figs 5, 8 and 9 for the ASAS counter, and similarly in Figs 4, 6 and 7 for the CSAS counter.

The exact calculations show a much more pronounced dip in the response curves for the  $4^\circ$  to  $22^\circ$  acceptance cone of the counters than is found for the *total* scattered energy. The effect, however, is the same. In the region of the dip, the counter necessarily lumps together particles of quite distinct sizes because they give the same response. This 'multi-valued' region is followed by a 'single-valued' region where the response does increase monotonically with size apart from the small-scale oscillations. The effect is that the particle size distribution inferred from measurements contains a 'knee' followed by a sharp drop. As has been emphasised in the foregoing discussion, and also in Ref 1, the position of the knee should depend on the aerosol refractive index.

### 3 RESULTS

We have made various sets of field measurements using these two Knollenberg aerosol counters which confirm the behaviour described. Here we use data taken at RAE Farnborough from 25 September to 3 October 1980, as the UK contribution to the collaborative aerosol measurement programme on and around the North Sea in Autumn 1980 under the auspices of NATO AC/243 Panel IV R.S.G.8. Our active probe, the ASAS-300, has four ranges covering 0.075 to 1.5  $\mu\text{m}$  nominal radius, while our classical high-volume probe, the CSAS-100-HV, has only two ranges covering 0.25 to 16  $\mu\text{m}$  nominal radius. The six ranges overlap considerably; the limits will be sufficiently clear from Fig 4 where the ranges, each

divided into 15 nominally equal size channels, are distinguished by different symbols. To ensure proper sampling, the probes were mounted on a frame which was controlled to point into the wind using a modified commercial aerial rotator system<sup>4</sup> slaved to a wind vane. The whole assembly was supported on a tripod with the probes about 2 m above ground level in a fairly flat grassy area.

Fig 4 shows a plot on a log-log scale of the particle size distribution  $n = dn/dr$  against  $r$  obtained from a period of autorange data, in which the probes cycle automatically through their ranges, on 29 September 1980. This example was deliberately chosen as the autorange period which shows the most marked knee - the drop occurs almost entirely between channels 9 and 10 of ASAS range 0, just at  $1 \mu m$  nominal size, and exceeds one order of magnitude. Where they overlap, the results from different ranges, particularly within the ASAS probe, are in excellent agreement. Also CSAS range 1 (symbol +) agrees well with ASAS range 0 (symbol \*), which it completely encompasses, and equally shows a large drop in imputed number density near  $1 \mu m$  although at much lower resolution. Usually the knee is less marked than in Fig 4 because the drop is spread over three or four channels perhaps due to a range of refractive indices. Even for a single refractive index, however, the drop should be spread over three channels if the knee is really in the middle of a channel rather than on the boundary between two channels.

Usually the probes were both operated on range 0, giving nearly continuous sampling of ASAS range 0 over 9 days. To get adequate statistics the data was then averaged hour by hour. As an automatic computational guide to the position of the knee, we simply found the ratios of the counts in successive channels and selected the largest ratio. The solid line at the top of Fig 5 shows the channel number preceding the knee as determined by this ratio method but with 12 changes made after visual inspection of the plots, the original values being shown by the symbol '+': in six instances the largest ratio is quite unconnected with the knee. Three times channel 14 is chosen by statistical vagary, twice channel 1 is chosen because there is a steep gradient at the bottom end of range 0 and the drop is spread over a few channels, and once channel 4 is chosen by a combination of these effects. There are also six minor changes in the last three days, where the drop is spread over a few channels and the largest drop is not the first one. The ratio method is thus not entirely successful, but no doubt a better algorithm could be devised. It is clear, however, that the position of the knee varies systematically with time.

Since the position of the knee ought to depend on the refractive index, it should therefore be correlated with relative humidity. Air temperature and dew point, and thus RH, were measured using an EG&G Model 220 Dew Point Hygrometer, and automatically recorded every 100 s. The lower curves in Fig 5 show the average RH over each hour together with the extreme values during the hour. Clearly the position of the knee does indeed correlate well with RH. Table 1 gives the correlation coefficients (i) using the channel number given by the ratio method, (ii) after making the obvious changes, and (iii) after making all changes. Values are given for the data overall, and also split



up into groups of 3 days. The obvious changes from channel 1 (twice) and channel 4 (once) have the greatest effect on the correlation, while the minor changes have almost no effect. Both the second and third groups of three days contain periods when both the external laser mirror in the ASAS probe and the misting mirror in the EG&G dew point sensor obviously warranted cleaning and duly were cleaned (see gaps in Fig 5); this must partly explain the lower correlations in Table 1. The correlation is extremely high, however, given that the position of the knee is quantised, that  $n_1$  is unlikely to depend linearly on RH, and that the presence of different substances could give distinctly different values of  $n_1$ .

Table 1

Correlation coefficient between the position (channel number) of the 'knee' on ASAS range 0 and the relative humidity based on measurements at RAE, Farnborough in September/October 1980. The number of changes is given in brackets

	25-27 September	28-30 September	1-3 October	Overall
Given by ratio method	0.627	0.454	0.807	0.610
After obvious changes	0.930 (2)	0.755 (2)	0.823 (2)	0.821 (6)
After all changes	0.930 (2)	0.755 (2)	0.852 (8)	0.844 (12)
Number of points	57	63	58	178

As shown in Fig 5, the lowest position for the knee is after channel 7 on 25 September when  $RH_{av}$  is 55.3% and on 26 September when  $RH_{av}$  is 61.6%. It clearly lies after channel 14 twice on 2 October when  $RH_{av}$  is 99.2% and 99.3%. In their Fig 13, Pinnick and Auvermann<sup>1</sup> give the results of *exact* calculations for the response of the ASAS counter to particles with  $m = 1.33 - 0i$  (water) and  $m = 1.50 - 0i$  (specifically ammonium sulphate but reasonably typical of other hygroscopic substances) assuming that the pulse height discriminator levels are set as recommended by the manufacturer. From their Fig 13, the knee should appear after channel 15 (for  $m = 1.33 - 0i$ ) and channel 7 (for  $m = 1.50 - 0i$ ) respectively on ASAS range 0. If our discriminator settings were also as recommended by the manufacturer, our highest and lowest knees correspond to refractive indices of about 1.35 and 1.50 respectively, by interpolation from the curves in Ref 1.

In Fig 4 further oscillations are evident on CSAS range 1 with peaks near 2  $\mu m$  and 3  $\mu m$  radius which correspond to the further oscillations in the scattering efficiency factor (see the topmost curve in Fig 6) which the counter cannot resolve on range 0. Specifically the peaks in Fig 4 should coincide with the portion between each maximum in Fig 6 and the succeeding minimum. These oscillations could likewise be used to find the refractive index for the relevant sizes of particle, but no analysis is attempted here since the range is sampled only occasionally in the present data. The oscillations on CSAS range 1 could also give some indication of the absorption since the corresponding

peaks in the scattering efficiency factor decrease with increasing absorption and have effectively vanished when  $n_2 \approx 0.1$  as shown in Fig 6. We have verified that the oscillations are not present if the counter is operated indoors in a low RH atmosphere when the aerosol particles will be solid, dusty and absorbing.

#### 4 CONCLUSIONS

We therefore conclude that the distortions imposed on the inferred particle size distribution by the characteristics of the counter responses are really an advantage in field measurements. The position of the knee on ASAS range 0 provides a good measurement of the refractive index (at the He-Ne wavelength) which could be put on an even sounder footing by regular electronic calibration or monitoring of the discriminator settings, etc. The distortions also provide a sensitive test that the probes are operating properly, and almost certainly could be adequately corrected for in the data analysis. In any case the distortions arise from the form of the scattering efficiency factor for particular ranges of particle size, and in practical terms seem unavoidable in an optical device.

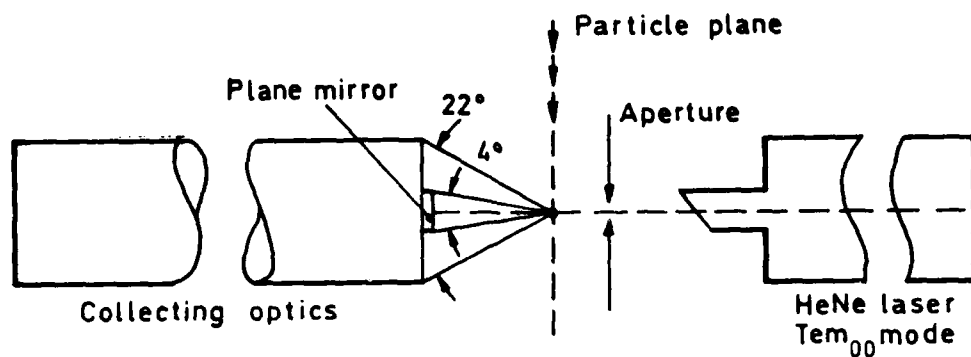
Pinnick and Auvermann<sup>1</sup> have suggested that channels should be aggregated together in preset groupings - no doubt a reasonable procedure if the refractive index is known and remains constant. With field measurements, however, any grouping of the channels should be done only after the position of the knee has been determined either from the size distribution or even by inferring the refractive index from the relative humidity.

If the results from the aerosol counters can be shown to be reliable, and if the sampling volume and discriminator settings are known, the results could be used to find the extinctions. Knowing the refractive index the real sizes of the particles could be found. At the same time the 'knee', and also the further oscillations if necessary, could be removed by curve-fitting. The extinctions at various different wavelengths could then be calculated. This Report is a step in that process.

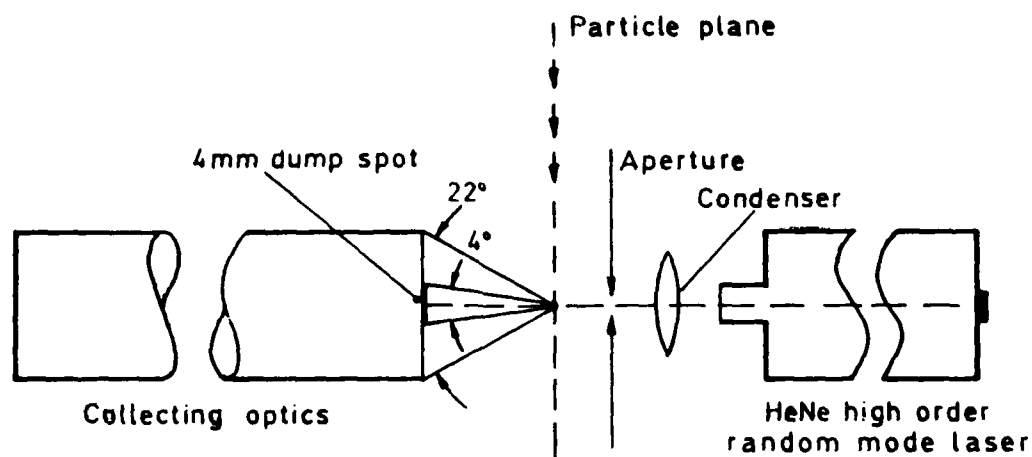
REFERENCES

- | <u>No.</u> | <u>Author</u>                  | <u>Title, etc</u>   |
|------------|--------------------------------|---|
| 1          | R.G. Pinnick<br>H.J. Auvermann | Response characteristics of Knollenberg light-scattering aerosol counters.<br><i>J. Aerosol Sci.</i> <u>10</u> , 55-74 (1979)                                     |
| 2          | M. Born<br>E. Wolf             | Principles of optics.<br>Third (revised) edition, p 662, Pergamon Press, Oxford (1965)  |
| 3          | J.V. Dave                      | Sub-routines for computing the parameters of the electromagnetic radiation scattered by a sphere.<br>IBM Palo Alto Scientific Center Report No.320-3237, May 1968 |
| 4          | R.C. Hughes<br>G.W. Stewart    | An aerosol probe rotator system.<br>RAE Technical Memorandum Space 283 (1981)   |

REV. 1.1 (25 OCT 1981) (RULY)  
LIC  
G. W. STEWART



a ASASP system



b CSASP system

Fig 1a&b Schematics of laser/optics systems

Fig 2

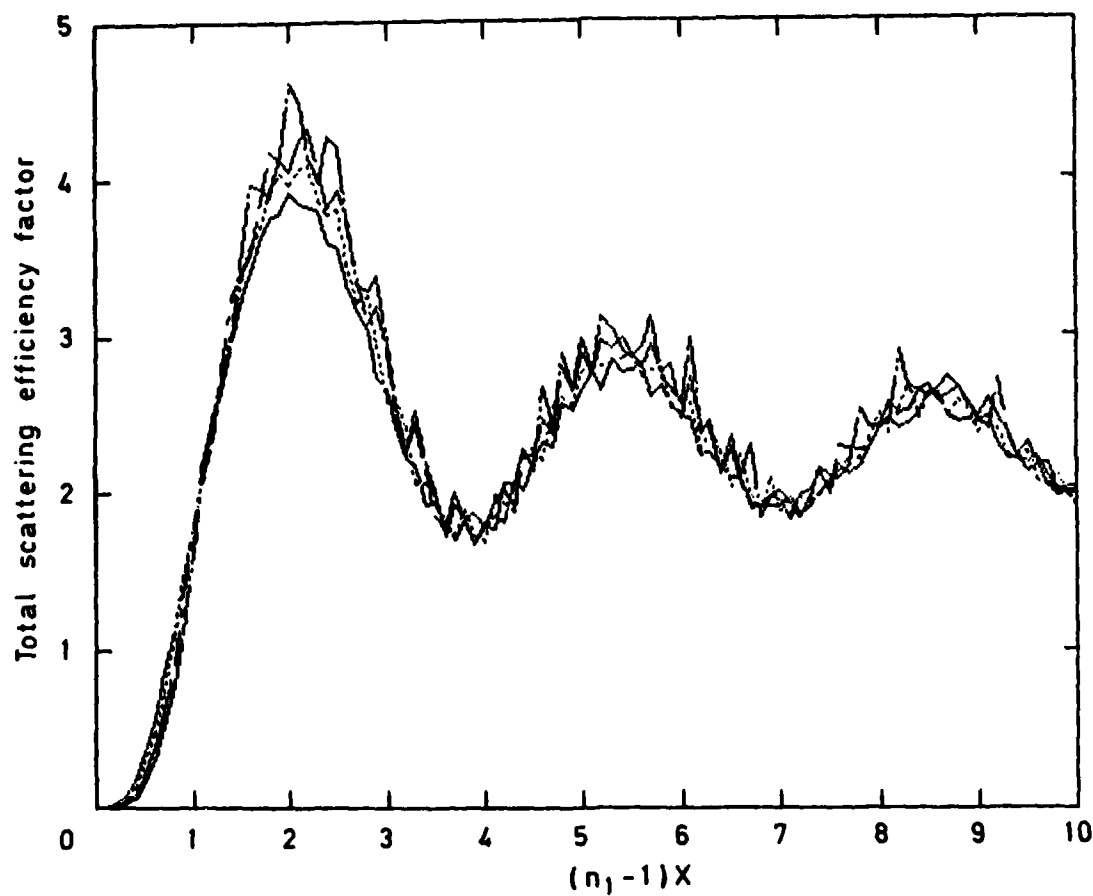


Fig 2 Total scattering efficiency factors for four values of refractive index,  $n_1 = 1.3, 1.4, 1.5, 1.6$ , and negligible absorption, plotted as functions of  $(n_1 - 1)X$ . The curves are not identified since the object is to show that they are nearly identical apart from small-scale oscillations

Fig 3

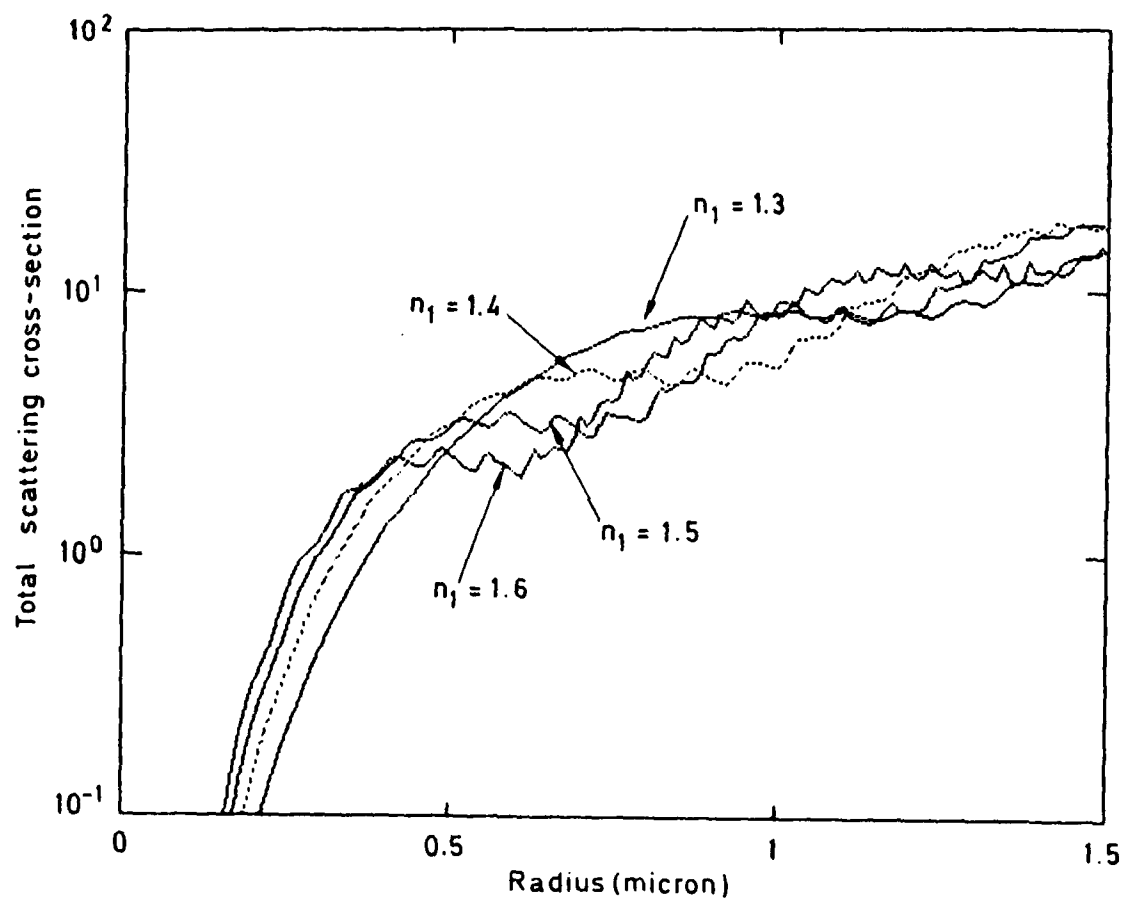


Fig 3 Total scattering cross-sections for four values of refractive index,  $n_1 = 1.3, 1.4, 1.5, 1.6$ , and negligible absorption

Fig 4

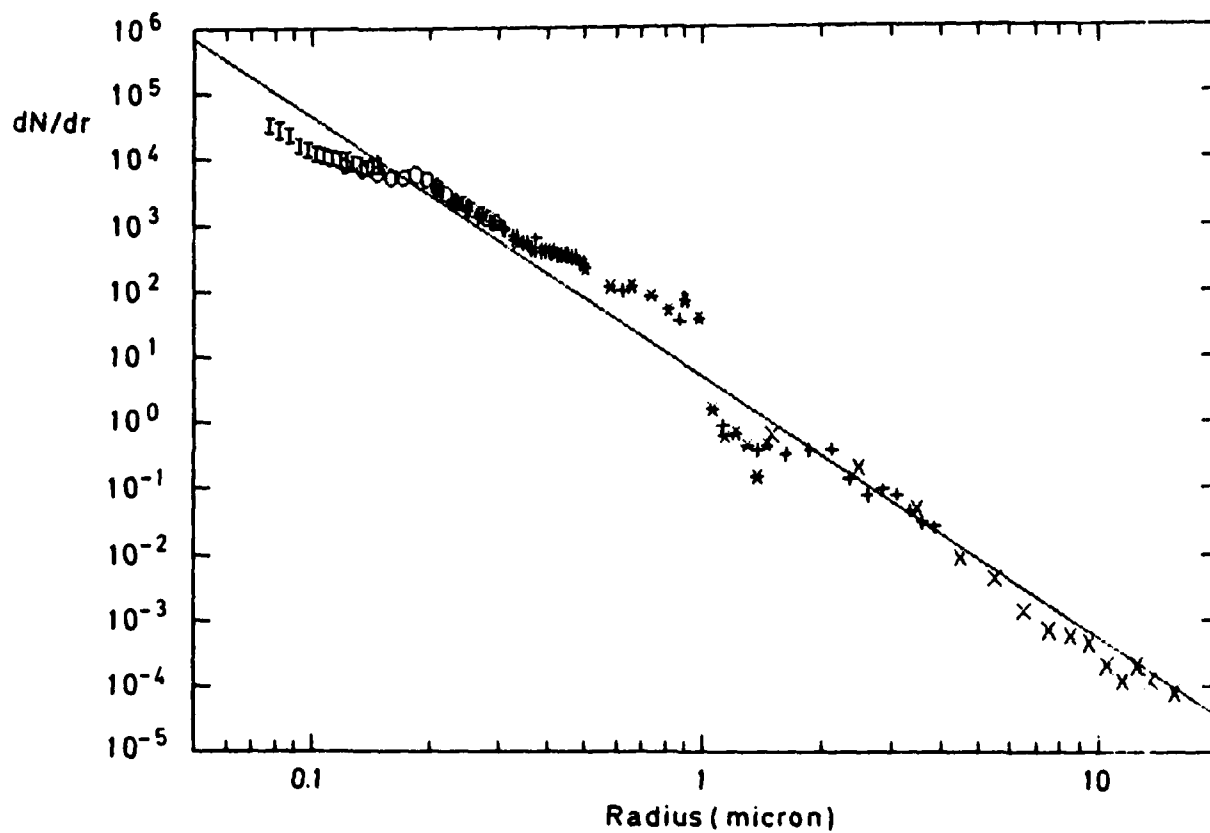


Fig 4 Particle size distribution from a period of autorange data on 29 September 1980, at RAE, Farnborough. Abscissa is the radius of the channel centre, and the symbols \* #, O, I, X, + are used for ranges 0 to 3 of the ASAS probe and ranges 0 and 1 of the CSAS probe respectively

Fig 5

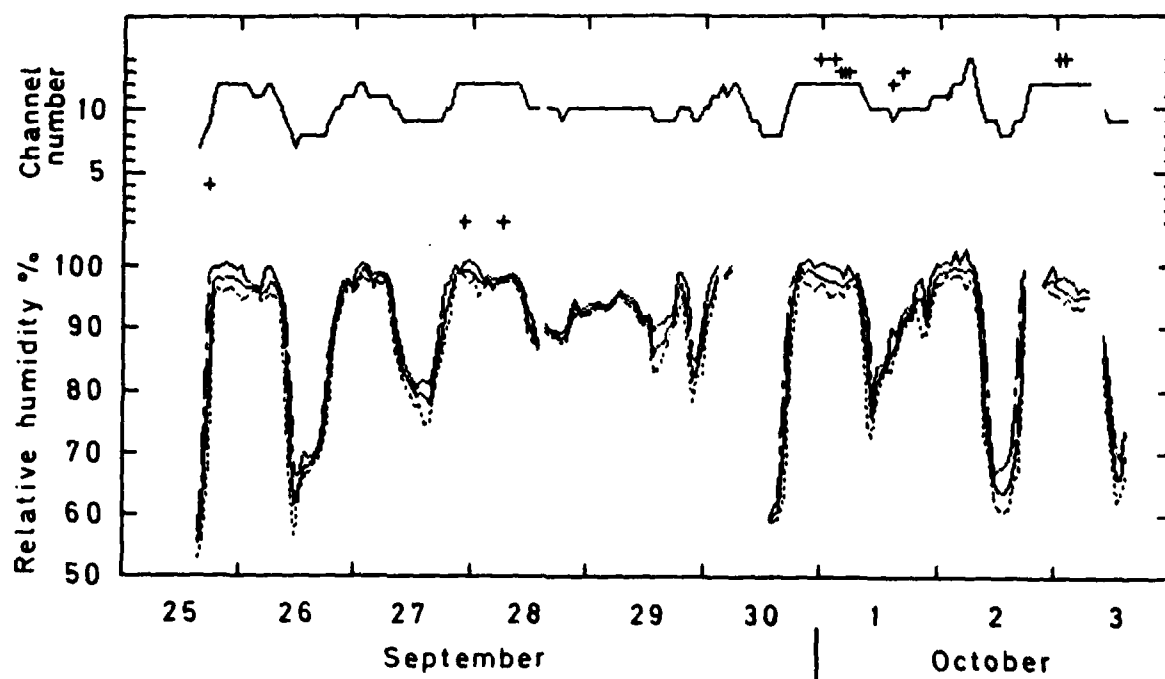


Fig 5 Time plot of the position of the knee on ASAS range 0 and the relative humidity (min, av, max) during hour. All data averaged over 1 hour



Fig 6

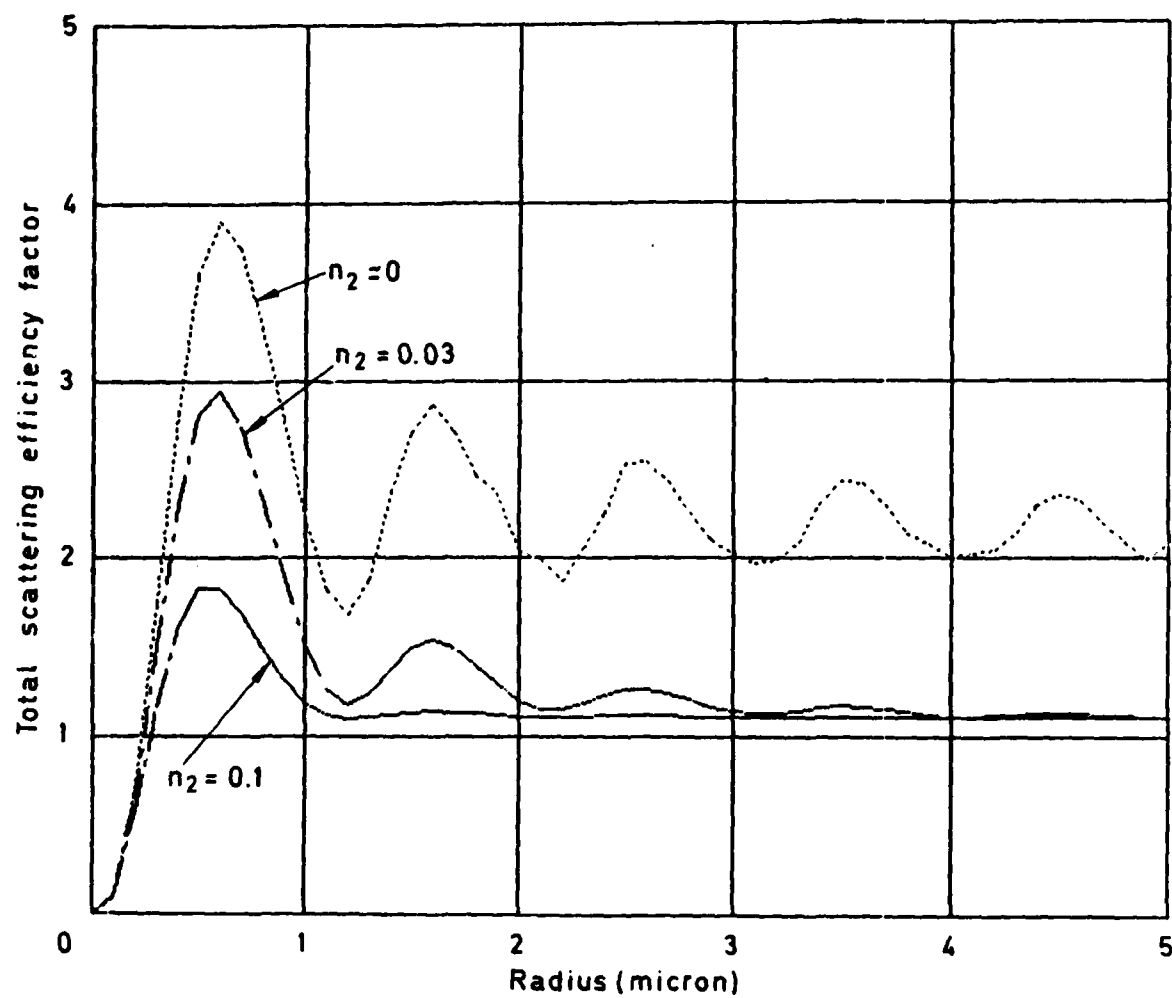


Fig 6 Total scattering efficiency factors with increasing absorption ( $\sim 0, 0.03, 0.1$ )

# REPORT DOCUMENTATION PAGE

Overall security classification of this page

UNCLASSIFIED

As far as possible this page should contain only unclassified information. If it is necessary to enter classified information, the box above must be marked to indicate the classification, e.g. Restricted, Confidential or Secret.

1. DRIC Reference (to be added by DRIC)	2. Originator's Reference RAE TR 82041	3. Agency Reference N/A	4. Report Security Classification/Marking UNCLASSIFIED		
5. DRIC Code for Originator 7673000W		6. Originator (Corporate Author) Name and Location Royal Aircraft Establishment, Farnborough, Hants, UK			
5a. Sponsoring Agency's Code N/A		6a. Sponsoring Agency (Contract Authority) Name and Location N/A			
7. Title On the response of Knollenberg aerosol counters					
7a. (For Translations) Title in Foreign Language					
7b. (For Conference Papers) Title, Place and Date of Conference					
8. Author 1. Surname, Initials Allan, R.R.	9a. Author 2 Ashdown, P.C.	9b. Authors 3, 4 ....		10. Date April 1982	Pages 14
11. Contract Number N/A		12. Period N/A		13. Project	
				14. Other Reference Nos. Space 615	
15. Distribution statement (a) Controlled by – (b) Special limitations (if any) –					
16. Descriptors (Keywords) (Descriptors marked * are selected from TEST) Aerosol counter. Natural aerosol. Refractive index.					

## 17. Abstract

It is known that the response of light-scattering aerosol counters is sensitive to the aerosol refractive index, and that even for a given refractive index there are 'multi-valued' regions where significantly different sizes of particle give the same response. In natural aerosols, the particle size distribution inferred directly from measurements shows a 'knee' followed by a sharp drop. Moreover the position of the knee should depend on the aerosol refractive index.

In practice the most obvious feature is a knee near 1  $\mu$ m nominal size on range 0 of the Knollenberg ASAS counter, although further features are present at much poorer resolution on range 1 of the Knollenberg CSAS counter. Here we show that the position of the knee correlates very well with relative humidity and thus with the refractive index. These 'artificial' features can be turned to advantage in field measurements of natural aerosol since they provide a measure of the refractive index.